JOURNAL OF SOLID STATE CHEMISTRY **105**, 573–579 (1993)

Relations between Oxygen Deficiency and Structures in the La–Sr–Cu–O System.
I. A New Oxygen-Deficient Phase, (La,Sr)$_5$Cu$_5$O$_{13}$

KENJI OTZSCHI, AKIHIKO HAYASHI, YOHKO FUJIWARA, AND YUTAKA UEDA

Institute for Solid State Physics, University of Tokyo, 7-22-1 Roppongi, Minato-ku, Tokyo 106, Japan

Received September 18, 1992; in revised form December 7, 1992; accepted December 8, 1992

A new compound in the La–Sr–Cu–O system was obtained by annealing $La_5SrCu_6O_{15}$ [or $(La_{0.8333}Sr_{0.1666})_8Cu_8O_{20}$ (8–8–20)] at 600°C under high O_2 pressure ($P_{O_2} = 300$ atm). It crystallizes in a tetragonal cell with parameters $a \approx \sqrt{5}a_p$ and $c \approx a_p$, in the same way as $La_4BaCu_5O_{13+\delta}$, where a_p means the cell constant of the cubic perovskite. By TG study the composition of this compound was estimated to be $(La_{0.8333}Sr_{0.1666})_5Cu_5O_{13.04\pm0.02}$ (5–5–13). The structure has been refined in the space group $P4/m$ by Rietveld analysis of powder X-ray diffraction. Lanthanum and strontium in the structure are statistically distributed, in contrast to $La_4BaCu_5O_{13+\delta}$, where lanthanum and barium are located in an ordered manner. The oxygen nonstoichiometry and the electrical resistivity of 8–8–20 and 5–5–13 compounds are also discussed.

1. Introduction

The cuprate oxides have been extensively investigated in the last several years since the discovery of high-T_c superconductors (*1*). Actually, copper can form a large family of ternary and quaternary oxides because of its ability to take mixed valences [Cu(I)–Cu(II)–Cu(III)] and various oxygen coordinations. It also shows a variety of physical properties which are very sensitive to oxygen nonstoichiometry.

The La–Ba–Cu–O system is a typical one, which contains so-called 214- and 123-superconductors and 415-metallic nonsuperconductors. The structures of these compounds are closely related to that of perovskite, in particular, $La_4BaCu_5O_{13+\delta}$ (415) has an oxygen-deficient perovskite structure with a characteristic arrangement of octahedral and pyramidal coordinate copper (*2*).

In the La–Sr–Cu–O system, another oxygen-deficient perovskite compound, $La_5SrCu_6O_{15-\delta}$ (516), has been synthesized. Its structure involves three types of copper coordination, octahedral, pyramidal, and square planar (*3*). This compound crystallizes in a tetragonal cell with parameters $a \approx 2\sqrt{2}a_p$ and $c \approx a_p$, where a_p is the parameter of the cubic perovskite, and has a wide solid-solution region from $x = 0.16$ to 0.24 in general formula $(La_{1-x}Sr_x)_8Cu_8O_{20-\varepsilon}$ (8–8–20). On the other hand, $La_4BaCu_5O_{13+\delta}$ has a tetragonal structure with lattice constants $a \approx \sqrt{5}a_p$ and $c \approx a_p$, and exists in a very narrow cation composition region around the stoichiometric composition (4–1–5), which shows a close relation between the structure and the metal (La and Ba) ordering.

It is worth investigating the relation between oxygen deficiency and structure or physical properties in order to understand a variety of copper oxides systematically. In this paper we report a new compound in

0022-4596/93 $5.00

the La–Sr–Cu–O system, $(La_{0.8333}Sr_{0.1666})_5Cu_5O_{13+\delta}$ (5–5–13), which was synthesized under high O_2 pressure. This newly found compound was similar to $La_4BaCu_5O_{13+\delta}$ in structure. We also report the structure as refined by Rietveld analysis and some physical properties of this compound. These compounds have an oxygen-vacancy ordered structure. Lanthanum and strontium in 5–5–13 are statistically distributed, in contrast to 4–1–5, where lanthanum and barium are located in an ordered manner.

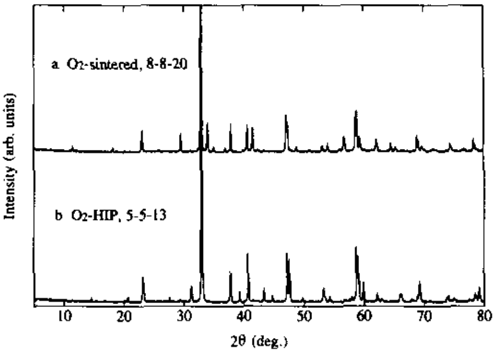

FIG. 1. X-ray powder diffraction pattern for (a) $(La_{0.8333}Sr_{0.1666})_8Cu_8O_{20}$ and (b) $(La_{0.8333}Sr_{0.1666})_5Cu_5O_{13}$.

2. Experimental

Starting samples, $(La_{1-x}Sr_x)_8Cu_8O_{20-\varepsilon}$ (x = 0.1666, 0.2, 0.2381, 0.25), were prepared by solid state reaction according to the published literature (*6*). Appropriate mixtures of predried La_2O_3, $SrCO_3$, and CuO were well ground and decarbonated in air at 900°C for 12 hr. Then the powders were reground, pressed into pellets, sintered under flowing oxygen (O_2-sintered) at 1025°C for 16 h, and finally cooled to room temperature slowly in the furnace. Regrinding and sintering were repeated several times until a homogeneous phase was obtained. Then the oxygenated sample was prepared by annealing the O_2-sintered sample (x = 0.1666) under 1500 atm (20% O_2/Ar, $P_{O_2} \approx 300$ atm) at 600°C for 6 hr (O_2-HIP (Hot Isostatic Pressing)).

Powder X-ray diffraction (XRD) measurements were carried out using a Mac Science MXP[18] system with a rotating anode generator and a monochromator of single-crystalline graphite for Cu*Kα* radiation. The Rietveld refinement was made on the O_2-HIP sample using the analysis program RIETAN (*9*) in the range 2θ = 20°–116°.

Thermogravimetric and differential thermal analysis were carried out using a Mac Science TG-DTA 2000 assembly under various atmospheres. The oxygen content was calculated from the weight loss by hydrogen reduction.

The electrical resistivity was measured by the ordinary four-probe method on O_2-sintered and -HIP pellet samples in the range 5–280 K at 1 K intervals. The magnetic susceptibility was measured by the conventional Faraday method at H = 11.8 kOe in the temperature range 4.2–300 K.

3. Results and Discussion

Figures 1a and b show XRD patterns of the O_2-sintered and -HIP samples, respectively. The pattern of the O_2-sintered sample, $(La_{1-x}Sr_x)_8Cu_8O_{20-\varepsilon}$, is as in (*6*); lattice constants at room temperature are a = 10.8606(4) Å and c = 3.8589(1) Å for x = 0.1666. The lattice constant variation with the strontium content x is given in Fig. 2.

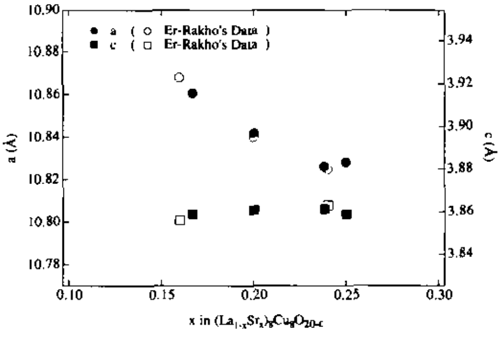

FIG. 2. Lattice constants for $(La_{1-x}Sr_x)_8Cu_8O_{20}$ as a function of strontium content x. Closed and open symbols represent our data and the data of Er-Rakho *et al.* (*3*), respectively.

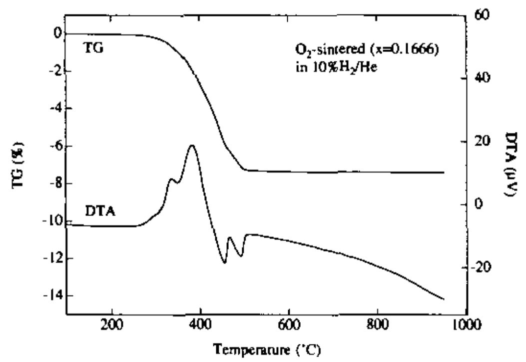

FIG. 3. TG and DTA curves for the O_2-sintered sample ($x = 0.1666$) heated at 5°C/min in flowing diluted hydrogen (10% H_2/He, 200 ml/min). The total weight loss is 7.41%.

Lattice constant a decreases and c slightly increases with increasing x, agreeing with the data of Er-Rakho *et al.* (*3*).

The XRD pattern of the O_2-HIP sample ($x = 0.1666$) is substantially different from that of the O_2-sintered samples and is similar to that of $La_4BaCu_5O_{13+\delta}$ (*6*). All the peaks in this pattern can be indexed on the basis of the same tetragonal cell as the 415 phase ($\sqrt{5}a_p \times \sqrt{5}a_p \times a_p$). The lattice parameters at room temperature are $a = 8.6160(1)$ Å, $c = 3.8226(1)$Å, which are slightly smaller than those of the 415 phase ($a = 8.66475(1)$Å, $c = 3.8594(1)$ Å), reflecting the smaller ion radius of strontium than of barium.

The thermogravimetric and differential thermal analysis (TG-DTA) was carried out to determine the oxygen content and the thermal decomposition in the O_2-sintered and -HIP samples. Figure 3 shows a TG-DTA curve for the O_2-sintered sample ($x = 0.1666$) heated at 5°C/min under flowing diluted hydrogen (10% H_2/He, 200 ml/min). The weight loss occurs between 300 and 500°C with some exothermic and endothermic peaks in the DTA curve; no more change is observed up to 960°C. Assuming that the compound was finally decomposed into a mixture of Cu metal, SrO, and La_2O_3, the total weight loss gives the composition $(La_{0.8333}Sr_{0.1666})_8Cu_8O_{20-\varepsilon}$ (or $La_5SrCu_6O_{15-\delta}$ in Tokura's notation), where the oxygen nonstoichiometry ε (or δ) is 0.00 ± 0.02. Er-Rakho *et al.* and Tokura *et al.* reported the larger values for the deficiency of oxygen, $\varepsilon = 0.08$ ($x = 0.16$) and $\delta = 0.1 \pm 0.1$ respectively, but our result is consistent with the stoichiometric $(La,Sr)_8Cu_8O_{20}$ structure. The slight difference between our result and their data possibly comes from the synthesis conditions, i.e., sintering temperature, atmosphere, cooling method etc.

Figure 4 shows the weight change of the O_2-sintered sample ($x = 0.1666$) in air. The observation under O_2 gas gave the same behavior. In the first elevation of temperature ((a) in Fig. 4), only a small weight loss is observed up to 1080°C and then a rapid change (−1.4%) occurs within about 20°C up to 1100°C with an endothermic peak in the DTA curve. This persistence of the weight at such a high temperature is consistent with the narrow range of oxygen deficiency. More temperature increase only gives a gradual decrease up to 1150°C. On cooling ((b) in Fig. 4), the sample gains weight, namely oxygen, with a step around 1030°C. This step is also observed reversibly in a second heating at about 1060°C ((c) in Fig. 4) with an endothermic peak. The resultant powder shows an XRD pattern which contains a 214 phase and CuO. The step

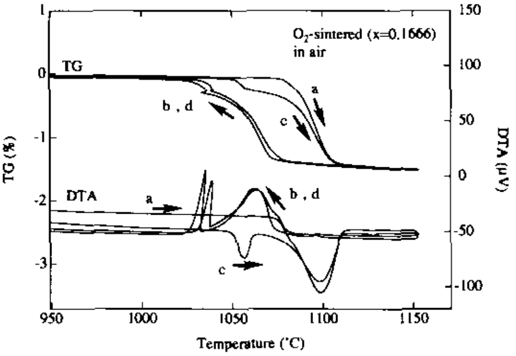

FIG. 4. TG and DTA curves for the O_2-sintered sample ($x = 0.1666$) heated/cooled at 5°C/min in air. The sample was heated to 1150°C in the first stage (a), then cooled to 850°C (b), reheated to 1150°C (c), and finally cooled to room temperature (d).

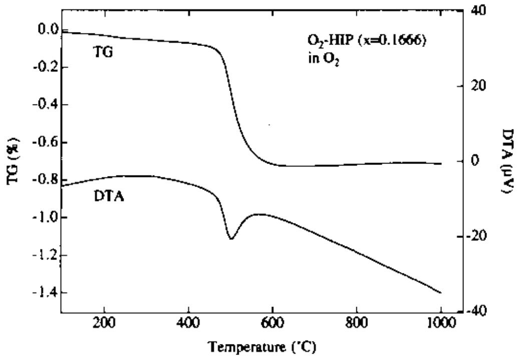

FIG. 5. TG and DTA curves for the O_2-HIP sample ($x = 0.1666$) heated at 10°C/min in flowing pure oxygen gas (99.9995%, 50 ml/min). The total weight loss is 0.73%.

around 1050°C may be caused by this decomposition. These results show that it would be difficult for the 8–8–20 phase to change into other more oxygen-deficient perovskite structures, $(La_{0.25}Sr_{0.75})_8Cu_8O_{18-\alpha}$ or $(La_{0.25}Sr_{0.75})_8Cu_8O_{16+\alpha}$ (4, 5), by the removal of oxygen. It decomposes into the stable 214 phase and CuO.

Reheating the O_2-HIP sample ($x = 0.1666$) under flowing oxygen gas results in a gradual decrease in weight up to 450°C and a drastic weight loss in the range 500–600°C with an endothermic peak in the DTA curve as shown in Fig. 5. The resultant powder shows the same XRD pattern as the O_2-sintered sample. From this weight loss the composition was estimated to be $(La_{0.8333}Sr_{0.1666})_5Cu_5O_{13.04\pm0.02}$ for the O_2-HIP sample. The similarity of the oxygen content between the 5–5–13 and 415 phases agrees with the result of XRD that both compounds have a similar structure, i.e., a similar oxygen-vacancy-ordered structure. Such low temperature of excess-oxygen release, however, suggests the instability of the 5–5–13 phase under ambient atmosphere, which is in contrast to $La_4BaCu_5O_{13+\delta}$. Kato *et al.* reported that δ is equal to 0 for the tetragonal form of this barium compound, and reduction in Ar atmosphere leads to the monoclinic $La_4BaCu_5O_{12.5}$ (*7*). On the other hand, it is a remarkable difference that the tetragonal 5–5–13 ($\sqrt{5}a_p \times \sqrt{5}a_p \times a_p$) phase shows a structural phase transition not to a monoclinic but to the tetragonal 8–8–10 ($2\sqrt{2}a_p \times 2\sqrt{2}a_p \times a_p$) phase.

From X-ray diffraction and TG measurements, this oxygenated sample was confirmed to be a new compound with composition $(La_{0.8333}Sr_{0.1666})_5Cu_5O_{13}$ and a structure similar to $La_4BaCu_5O_{13}$. Then we tried to refine the structure using Rietveld analysis. The structure refinement was carried out in the same space group, *P*4/*m*, as $La_4BaCu_5O_{13}$ for the powder X-ray diffraction pattern. Calculations were started with the same atomic positions as $La_4BaCu_5O_{13}$ and the atomic parameters after final refinement are given in Table I. The discrepancy factor is calculated to be $R_i = 0.0274$ ($R_p = 0.0476$; $R_e = 0.0318$; $R_{wp} = 0.0650$). The most striking result is that lanthanum and strontium are statistically distributed over 1(*d*) and 4(*k*) sites while in $La_4BaCu_5O_{13}$ lanthanum and barium are strictly located on the 1(*d*) and 4(*k*) sites respectively (*2*). Refining with variable occupation factors of lanthanum and strontium on these sites made no differences on the discrepancy factor and the atomic parameters, and the occupation factors became to be consistent with the statistical distribution within the standard deviations. This result suggests that the oxygen content rather than the ordering of metals (La and Ba or Sr) is essential for 4–1–5 structure ($\sqrt{5}a_p \times \sqrt{5}a_p$). This disorder of

TABLE I

REFINED ATOMIC PARAMETERS OF $(La_{0.8333}Sr_{0.1666})_5Cu_5O_{13}$ (SPACE GROUP *P*4/*m*)

Atom	Site	*x*	*y*	*z*
La(Sr)(1)	1(d)	0.5	0.5	0.5
La(Sr)(2)	4(k)	0.1325(5)	0.2753(5)	0.5
Cu(1)	1(a)	0	0	0
Cu(2)	4(j)	0.420(1)	0.174(1)	0
O(1)	1(b)	0	0	0.5
O(2)	4(j)	0.275(4)	0.393(4)	0
O(3)	4(j)	0.230(6)	0.040(4)	0
O(4)	4(k)	0.417(4)	0.176(4)	0.5

TABLE II

INTERATOMIC DISTANCES IN $(La_{0.8333}Sr_{0.1666})_5Cu_5O_{13}$

M–O		Distance (Å)
Cu(1)–O(1)[a]	×2	1.9113(0)
Cu(1)–O(3)[a]	×4	2.003(9)
Cu(2)–O(2)[a]	×1	2.256(6)
Cu(2)–O(2)[b]	×1	1.832(6)
Cu(2)–O(3)[a]	×1	2.034(9)
Cu(2)–O(4)[a]	×2	1.9115(1)
La(Sr)(1)–O(2)[a]	×8	2.873(5)
La(Sr)(1)–O(4)[a]	×4	2.882(7)
La(Sr)(2)–O(1)[a]	×1	2.6322(9)
La(Sr)(2)–O(2)[a]	×2	2.488(4)
La(Sr)(2)–O(3)[a]	×2	2.941(4)
La(Sr)(2)–O(3)[b]	×2	2.426(3)
La(Sr)(2)–O(4)[a]	×2	2.598(6)
La(Sr)(2)–O(4)[c]	×1	2.676(6)
La(Sr)(2)–O(4)[b]	×1	2.925(7)

Note. Symmetry codes: [a] x, y, z; [b] $-y, x, z$; [c] $y, 1-x, z$

La and Sr may be due to the close ion radius of 12-coordinate strontium (1.58 Å) to lanthanum (1.50 Å), while barium (1.75 Å) is far larger than these cations.

Distances between metal and oxygen atoms are shown in Table II (see also Fig. 6). All values are compatible with those usually observed in cuprate oxides. The $Cu(1)O_6$ octahedra are somewhat compressed along the *c* axis, as usually observed, and the $Cu(2)O_5$ pyramids have four shorter Cu–O distances (1.83–2.03 Å) and one longer Cu–O distance (2.26 Å) which is *trans* to the oxygen vacancy. La(Sr)(1) (1(*d*) site) is surrounded by twelve oxygen atoms which are located in the average distances (O(2) : 2.87 Å × 8, O(4) : 2.88 Å × 4). These close values contrast with the slightly different distances in $La_4BaCu_5O_{13+\delta}$ (O(2) : 2.93 Å, O(4) : 3.06 Å), where the 1(*d*) site is occupied by a larger barium ion, and oxygen atoms in the 4(*k*) site (O(4)) lie farther apart from this cation and are no longer right over Cu(2). The arrangement of oxygen atoms around La(Sr)(2) is more interesting because it is distorted according to the oxygen vacancy. O(2) and O(3) move to the vacancy (Fig. 6) and this polyhedron has four La(Sr)–O distances (2.43 and 2.49 Å) shorter than the other eight (2.60–2.94 Å). And because of this distortion, CuO_6 octahedra and CuO_5 pyramids rotate in directions opposite each other (Fig. 6).

The resistivity data of the O_2-sintered (x = 0.1666, 0.2000, 0.2381, and 0.2500) and -HIP (x = 0.1666) samples are shown in Fig. 7. All samples are mostly metallic (the anomaly for x = 0.1666 near 40 K is due to the superconducting second phase, which can be negligible in amount). The resistivity of $(La_{1-x}Sr_x)_8Cu_8O_{20}$ (O_2-sintered) tends to decrease with increasing strontium concentration. And the anomaly for x = 0.1666 around 230 K shifts to higher temperature with decreasing strontium concentration in agreement with Tamegai's results (150 K for x = 0.2000, 200 K for x = 0.1838)

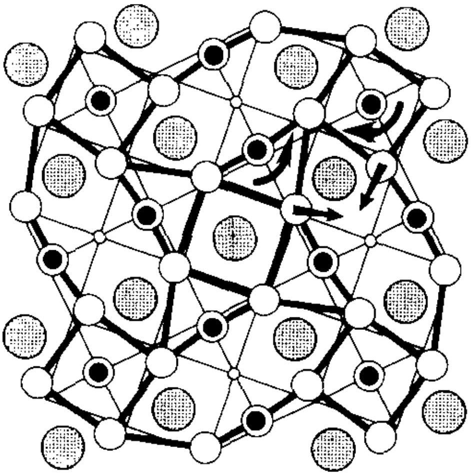

FIG. 6. Schematic projection of the framework of $(La_{0.8333}Sr_{0.1666})_5Cu_5O_{13}$ onto the (001) plane. Large shaded and small closed circles mean the cations La(Sr) and Cu, respectively. Large open circles stand for oxygen atoms, while small open ones represent oxygen vacancies. Thin lines represent ideal cubic perovskite. Each atom is located off the ideal position, and oxygen atoms (O(2) and O(3)) move toward the oxygen vacancy (arrows). CuO_6 octahedra and CuO_5 pyramids (represented by thick lines) rotate in the opposite direction from each other in accordance with these oxygen movements (curved arrows).

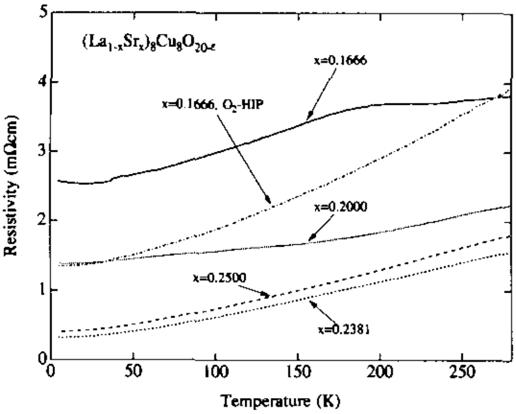

FIG. 7. Temperature dependence of electric resistivity for each O_2-sintered and -HIP sample. O_2-sintered: $x = 0.1666$ (solid line), 0.2000 (small dotted), 0.2381 (large dotted), and 0.2500 (dashed); O_2-HIP: $x = 0.1666$ (dashed-dot). An anomaly around 40 K for the O_2-sintered ($x = 0.1666$) is caused by small quantities of a superconducting second phase. Measurements down to 5 K show no evidence of superconductivity for any of the compounds above.

(*8*). The oxygenated $(La_{0.8333}Sr_{0.1666})_5Cu_5O_{13}$ is free from this anomaly as well as $La_4BaCu_5O_{13}$ but this anomaly has been observed in the monoclinic reduced $La_4BaCu_5O_{12.5}$ (*7*). The average valence of copper is affected by both strontium concentration and oxygen content. We have no explanation for the anomaly of the resistivity curves but it can be said from these results that the lower carrier concentration or the lower average valence of copper would be responsible for the anomaly.

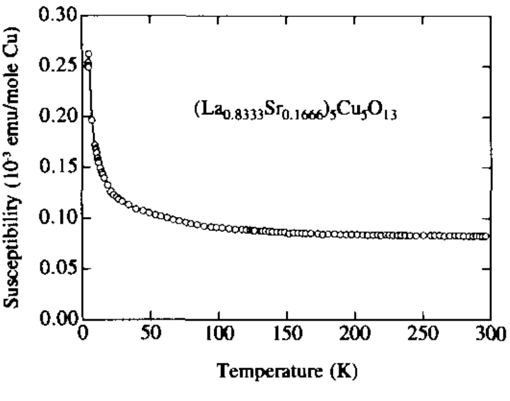

FIG. 8. Magnetic susceptibility of $(La_{0.8333}Sr_{0.1666})_5Cu_5O_{13}$ as a function of temperature.

The temperature dependence of the magnetic susceptibility of $(La_{0.8333}Sr_{0.1666})_5Cu_5O_{13}$ is shown in Fig. 8. It shows the same Pauli paramagnetic nature and weak temperature dependence as other strontium or barium cuprates, 8–8–20, 2–1–2–6 and 4–1–5 (*10*). The increase as decreasing temperature is due to the existence of the magnetic impurities.

4. Concluding Remarks

We have succeeded in synthesizing a new phase $(La_{1-x}Sr_x)_5Cu_5O_{13}$ ($x = 0.1666$) in the La–Sr–Cu–O system by annealing $(La_{1-x}Sr_x)_8Cu_8O_{20}$ ($x = 0.1666$) under high O_2 pressure. This new compound has the same structure as $La_4BaCu_5O_{13}$ but lanthanum and strontium in the structure are distributed in a disordered manner, in contrast to the case of La and Ba in $La_4BaCu_5O_{13}$. This difference between these two compounds may be caused by that of the ion radii between strontium and barium. This result suggests that the structure of 5–5–13 ($\sqrt{5}a_p \times \sqrt{5}a_p \times a_p$) would depend on the oxygen content rather than the concentration ratio of La and Ba or Sr. The wide solid solution region in La–Sr–Cu–O system may be due to the similar ion size of strontium to that of lanthanum. Now we are researching the single phase range of the 5–5–13 compound with varying x and oxygen deficiency of the 8–8–20 compound.

Acknowledgments

The authors thank Mr. K. Shibutani and Mr. R. Ogawa (Kobe Steel, Ltd.) for high pressure treatments. They are grateful to Mr. K. Koga for measurement of magnetic susceptibility. One of them is extremely grateful to Dr. S. Kambe for fruitful discussion. This work was partly supported by a Grant-in-Aid for Scientific Research on Priority Areas, "Science of High T_c Superconductivity," given by the Ministry of Education, Science, and Culture of Japan.

References

1. J. G. Bednorz and K. A. Muller, *Z. Phys. B* **64,** 189 (1986).
2. C. Michel, L. Er-Rakho, M. Hervieu, J. Pannetier, and B. Raveau, *J. Solid State Chem.* **68,** 143 (1987).
3. L. Er-Rakho, C. Michel, and B. Raveau, *J. Solid State Chem.* **73,** 514 (1988).
4. W. T. Fu, F. C. Mijlhoff, D. J. W. Ijdo, and V. Ponec, *Solid State Commun.* **83,** 59 (1992).
5. H. Fujishita, M. Sera, and M. Sato, *Physica C* **175,** 165 (1991).
6. Y. Tokura, J. B. Torrance, A. I. Nazzal, T. C. Huang, and C. Ortiz, *J. Am. Chem. Soc.* **109,** 7555 (1987).
7. M. Kato, N. Kojima, K. Yoshimura, Y. Ueda, N. Nakayama, and K. Kosuge, *J. Solid State Chem.* **103,** 253 (1993).
8. T. Tamegai and Y. Iye, *Physica C* **159,** 181 (1989).
9. F. Izumi, *J. Crystallogr. Soc. Jpn.* **27,** 23 (1985).
10. J. B. Torrance, Y. Tokura, A. Nazzal, and S. S. P. Parkin, *Phys. Rev. Lett.* **60,** 542 (1988).